0026-895X/07/7201-112–120$20.00
MOLECULAR PHARMACOLOGY
Copyright © 2007 The American Society for Pharmacology and Experimental Therapeutics
Mol Pharmacol 72:112–120, 2007

Vol. 72, No. 1
33761/3222841
Printed in U.S.A.

Adrenomedullin Stimulates Nitric Oxide Production from Primary Rat Hypothalamic Neurons: Roles of Calcium and Phosphatases

Yong Xu and Teresa L. Krukoff

Department of Cell Biology and Center for Neuroscience, Faculty of Medicine and Dentistry, University of Alberta, Edmonton, Alberta, Canada

Received January 1, 2007; accepted April 18, 2007

ABSTRACT

Adrenomedullin (ADM) in the brain plays important roles in the maintenance of homeostasis. Although in vivo evidence has suggested that nitric oxide (NO) mediates ADM's effects in the brain, mechanisms for ADM stimulation of NO production in neurons have not been identified. In the present study, primary hypothalamic neurons were used to characterize ADM-induced NO production and to study the underlying mechanisms. Using Calcium Orange/4-amino-5-methylamino-2′,7′-difluorofluorescein fluorescence live cell imaging, we found that ADM (1 or 10 nM, 5 min) significantly elevated $[Ca^{2+}]_i$ and NO production in a concentration-dependent manner. Ca^{2+} and NO responses induced by 10 nM ADM were abolished by pretreatment with 50 μM 1,2-bis(2-aminophenoxy)ethane-*N*,*N*,*N*′,*N*′-tetraacetic acid-acetoxymethyl ester (BAPTA-AM), an intracellular Ca^{2+} chelator, or protein kinase A (PKA) inhibitors 5 μM *N*-[2-(*p*-bromocinnamylamino)ethyl]-5-isoquinolinesulfonamide dihydrochloride (H-89) and 50 μM Rp-cAMP. Furthermore, the ADM-induced NO production was significantly attenuated by a protein phosphatase 1/2A inhibitor, okadaic acid (OA; 0.1 μM), or calcineurin inhibitors, tacrolimus (FK506) (1 μM) and cyclosporin A (CsA; 0.1 μM). Using Western blotting, we found that ADM significantly decreased phosphorylation of neuronal nitric-oxide synthase (nNOS) at serine 847. This dephosphorylation was inhibited by 0.1 μM OA, 1 μM FK506, 0.1 μM CsA, or 5 μM H-89, and attenuated by 50 μM BAPTA-AM. These results suggest that, in hypothalamic neurons, ADM elevates $[Ca^{2+}]_i$ via PKA-associated mechanisms. The PKA/Ca^{2+} cascade leads to protein phosphatase (PP) 1/PP2A- and calcineurin-mediated dephosphorylation of nNOS. We hypothesize that the Ca^{2+} increase and nNOS dephosphorylation contribute to activation of nNOS and production of NO in hypothalamic neurons.

Adrenomedullin (ADM), a 52 amino acid peptide, was first isolated from human pheochromocytoma in 1993 (Kitamura et al., 1993). ADM in peripheral tissues plays important roles in regulating vascular tone, cardiac output, and renal functions, and systemic infusion of ADM has therapeutic effects on hypertension, myocardial infarction, and heart and renal failure (Ishimitsu et al., 2006). In addition to its actions in the periphery, ADM contributes extensively to the maintenance of homeostasis through central mechanisms. Thus, centrally administered ADM inhibits thirst and salt appetite (Taylor et al., 2005), suppresses food intake (Taylor et al., 1996), and regulates blood pressure, heart rate, and baroreflex sensitivity by modulating autonomic activity (Shan and Krukoff, 2001; Xu and Krukoff, 2004a,b, 2006).

Although the molecular mechanisms for ADM's action in the brain remain unclear, evidence from our laboratory suggests that nitric oxide (NO), a nonconventional neurotransmitter in the central nervous system (Krukoff, 1999), is an important mediator of ADM's actions in the brain. For example, ADM activates NO-producing neurons in the hypothalamic paraventricular nucleus (PVN) and stimulates NO production in the hypothalamus (Shan and Krukoff, 2001). In addition, the hypotensive effects induced by microinjections

This work was supported by the Heart and Stroke Foundation of Alberta/Northwest Territories/Nunavut. Y.X. is the recipient of a studentship from the Heart and Stroke Foundation of Canada.

Article, publication date, and citation information can be found at http://molpharm.aspetjournals.org.

doi:10.1124/mol.106.033761.

ABBREVIATIONS: ADM, adrenomedullin; BAPTA-AM, 1,2-bis(2-aminophenoxy)ethane-*N*,*N*,*N*′,*N*′-tetraacetic acid-acetoxymethyl ester; Ca^{2+}-CaM, Ca^{2+}-calmodulin complex; CaMKII, calmodulin-dependent kinase II; CRLR, calcitonin receptor-like receptor; MEM, minimum essential medium; NMDA, *N*-methyl-D-aspartate; NOS, nitric-oxide synthase; nNOS, neuronal nitric-oxide synthase; NOSIP, nitric-oxide synthase interaction protein; PVN, paraventricular nucleus; RAMP-2/3, receptor-activity-modifying protein 2 or 3; H-89, *N*-[2-(*p*-bromocinnamylamino)ethyl]-5-isoquinolinesulfonamide dihydrochloride; FK506, tacrolimus; DAF-FM, 4-amino-5-methylamino-2′,7′-difluorofluorescein; PKA, protein kinase A; OA, okadaic acid; CsA, cyclosporin A; PBS, phosphate-buffered saline; vinyl-L-NIO, N^5-(1-imino-3-butenyl)-ornithine; PP1, protein phosphatase 1.

of ADM into the PVN are attenuated by inhibition of NO synthesis (Xu and Krukoff, 2004b). Likewise, the NO-cGMP cascade mediates ADM's hypertensive effects in the rostral ventrolateral medulla, an autonomic center in the brainstem that participates in maintaining sympathetic tone (Xu and Krukoff, 2004a). Finally, we demonstrated a direct stimulatory effect of ADM on NO production in SK-N-SH human neuroblastoma cells in vitro (Xu and Krukoff, 2005). However, the mechanisms by which ADM stimulates NO production in primary neurons remain to be identified.

NO production in neurons is catalyzed by neuronal nitric-oxide synthase (nNOS), and multiple mechanisms are involved in the regulation of nNOS activity. A transient increase in $[Ca^{2+}]_i$ leads to the formation of the Ca^{2+}-calmodulin complex (Ca^{2+}-CaM), which, in turn, binds to and activates nNOS by regulating intersubunit electron transfer and oxygen activation (Panda et al., 2001). In addition, nNOS is phosphorylated and therefore regulated by various kinases, including protein kinase A (PKA), protein kinase C, cGMP-dependent kinase, and calmodulin-dependent kinase II (CaMKII) (Bredt et al., 1992; Dinerman et al., 1994; Komeima et al., 2000). In particular, phosphorylation of nNOS at serine 847 suppresses the binding of nNOS with Ca^{2+}-CaM and decreases the catalytic activity of the enzyme (Komeima et al., 2000). On the other hand, protein phosphatases, such as protein phosphatase 1 (PP1), protein phosphatase 2A (PP2A), and calcineurin (also known as protein phosphatase 2B), reverse this inhibitory phosphorylation and stimulate nNOS activity (Rameau et al., 2003).

In the present study, primary rat hypothalamic neurons were used as a model to investigate the mechanisms by which ADM stimulates NO production in neurons. Expression of ADM receptor components, calcitonin receptor-like receptor (CRLR) and receptor-activity-modifying protein 2 or 3 (RAMP-2/3) (McLatchie et al., 1998), was first characterized in the hypothalamic neurons, and nNOS expression was then demonstrated in putative ADM-responsive neurons. Effects of ADM on Ca^{2+} dynamics, NO production, and nNOS phosphorylation were then examined. Furthermore, various pharmacological agents were used to determine the involvement of ADM receptors, nNOS, protein phosphatases, Ca^{2+} signaling, and the cAMP-PKA pathway in ADM's effects.

Materials and Methods

Cell Culture. Primary hypothalamic neurons were cultured using a modified protocol based on a previous study (Boyadjieva et al., 2003). In brief, in a sterile environment, pregnant Sprague-Dawley rats on days 17 to 18 of gestation were anesthetized with Halothane (Halocarbon Laboratories, River Edge, NJ), embryos were surgically removed from the mothers, and brains were removed from the embryos. Hypothalami were dissected anteriorly, ~1 mm rostral to the optic chiasm; posteriorly, at the rostral extent of the mammillary bodies; and laterally, at the hypothalamic sulci. The depth of the excised tissue was approximately 2 mm. The hypothalami were dissected in Hanks' balanced salt solution supplemented with 15 mM HEPES, 10 U/ml penicillin, and 10 mg/ml streptomycin, digested with 0.05% trypsin for 15 min, triturated, and then plated in 6- or 96-well culture plates or 12- or 40-mm diameter coverslips coated with 10 mg/ml poly(D-lysine) (Sigma-Aldrich, St. Louis, MO). The cultures were grown at 37°C in a 5% CO_2 humidified atmosphere, and the medium was changed every 2 days. Neurobasal medium supplemented with 10% fetal bovine serum, N2 supplement, 15 mM HEPES, 1.5 mM sodium pyruvate, 30 U/ml penicillin, 30 μg/ml streptomycin, and 0.6 mM glutamine was used as culture medium for the first 2 days; on the third day, glutamine was substituted by 10 nM cytosine arabinoside (Sigma-Aldrich). On day 5, fetal bovine serum was removed from the culture medium. All reagents for cell culture, except when otherwise mentioned, were purchased from Invitrogen (Burlington, ON, Canada). Using antibodies for microtubule-associated protein-2 (GeneTex, San Antonio, TX) and for glial fibrillary acidic protein (Santa Cruz Biotechnology, Santa Cruz, CA), we determined that in 10-day cultures, approximately 90% of cells are neurons, and approximately 1% of the population is composed of astrocytes. Thus, experiments described below were performed with cells from day 10 or day 11 cultures.

Immunocytochemistry. Cells cultured on 12-mm diameter coverslips (2×10^5 cells/coverslip) were fixed with 3% paraformaldehyde for 20 min and air-dried. The coverslips were then incubated in 0.1% Triton X-100 in PBS for 4 min followed by three washes with 0.2% gelatin (Fisher Scientific, Nepean, ON, Canada) in PBS. The coverslips were incubated with 1:500 goat anti-CRLR together with 1:500 rabbit anti-RAMP-2, 1:500 rabbit anti-RAMP-3, or 1:500 rabbit anti-nNOS (all from Santa Cruz) for 1.5 h, followed by 1-h incubation of 1:200 Cy3-conjugated donkey anti-goat IgG and 1:200 biotinylated donkey anti-rabbit IgG (both from Jackson ImmunoResearch Laboratories). Finally, coverslips were incubated in Streptavidin-Alexa 488 (1:200; both from Jackson ImmunoResearch Laboratories, Inc., West Grove, PA) for 1 h. After washing three times with PBS, the coverslips were mounted with 4′-6-diamidino-2-phenylindole (Vector Laboratories, Inc., Burlingame, CA) and sealed on glass slides. Expression of proteins was observed with a fluorescence confocal microscope.

Calcium Orange/DAF-FM Fluorescent Live Cell Imaging. To simultaneously monitor intracellular Ca^{2+} dynamics and NO production, hypothalamic neurons cultured on 40-mm glass coverslips ($0.5–1 \times 10^6$ cells/coverslip) were incubated with minimum essential medium (MEM) containing 10 μM Calcium Orange (Invitrogen), a fluorescent Ca^{2+} indicator (Prendergast et al., 2004), and 3.5 μM DAF-FM (Invitrogen), a fluorescent NO indicator (Shao et al., 2003), for 60 min at 37°C followed by a 30-min postincubation period in MEM without the fluorescent indicators. Coverslips were then assembled in the Focht Chamber System 2 (Bioptechs, Butler, PA), which was mounted on a Carl Zeiss laser scanning microscope (European Molecular Biology Laboratory, Heidelberg, Germany). The temperature in the chamber was maintained at 37°C with an objective heat controller (Bioptechs). Red fluorescence from Calcium Orange (at excitation and emission wavelengths of 543 and 560 nm, respectively) and green fluorescence from DAF-FM (at excitation and emission wavelengths of 488 and 515 nm, respectively) were recorded every 50 s.

At the beginning of each experiment, MEM was added into the chamber, and cells were allowed to rest for at least 5 min to obtain basal fluorescence levels. To characterize the effects of ADM on $[Ca^{2+}]_i$ and NO production, MEM containing ADM (1 or 10 nM; American Peptide Company, Sunnyvale, CA) was injected into the chamber; the solution was washed away with MEM 5 min later. To determine which receptor mediates ADM's effects, cells were first exposed to 10 nM ADM for 5 min, washed with MEM, and then pretreated for 10 min with 10 nM $ADM_{22–52}$, a putative antagonist for ADM receptor composed of CRLR and RAMP-2 or 10 nM $CGRP_{8–37}$, a putative antagonist for CGRP receptor or ADM receptor composed of CRLR and RAMP-3 (Hay et al., 2004). These pretreatments were then followed by 5-min applications of 10 nM ADM in the presence of respective antagonists. Likewise, various pharmacological agents, including 2 μM N^5-(1-imino-3-butenyl)-ornithine (vinyl-L-NIO, a selective nNOS inhibitor; Alexis Corporation, San Diego, CA) (Xu and Krukoff, 2005), 50 μM BAPTA-AM, an intracellular Ca^{2+} chelator) (Xu and Krukoff, 2005), 5 μM H-89 (a PKA inhibitor) (Xu and Krukoff, 2005), 50 μM Rp-cAMP (a PKA inhibitor) (Dong and White, 2003), 0.1 μM okadaic acid (OA, a PP1/PP2A inhibitor) (Rameau et al., 2003), 1 μM FK506 (tacrolimus, a calcineurin inhib-

itor) (Rameau et al., 2003) or cyclosporin A (CsA, a calcineurin inhibitor; all from Sigma-Aldrich) (Rameau et al., 2003), were used to evaluate the contributions of nNOS, Ca^{2+}, PKA, and protein phosphatases, respectively, in the ADM-induced responses. In control experiments, MEM was injected into the chamber at corresponding time points. Fluorescence intensity from each cell was quantified over time using LSM 510 software (European Molecular Biology Laboratory), and relative $[Ca^{2+}]_i$ and NO levels were represented as the ratios of fluorescence intensities to their respective basal levels (F/F_0).

Measurement of Intracellular cAMP by EIA. As described previously (Xu and Krukoff, 2005), cells (grown at a density of 10^5/well in 96-well culture plates) were treated with 0.5 mM 1-methyl-3-isobutylxanthine (a cyclic nucleotide phosphodiesterase inhibitor; Sigma-Aldrich) for 30 min to prevent breakdown of accumulated cAMP, followed by treatment with vehicle, 1 or 10 nM ADM, for 5 min. Intracellular cAMP levels were measured with a commercial enzyme immunoassay kit according to the manufacturer's instructions (GE Healthcare, Chalfont St. Giles, Buckinghamshire, UK).

Phosphorylation of nNOS Analyzed with Western Blotting. To illustrate the dose-response of the ADM-induced nNOS dephosphorylation in hypothalamic neurons, cells cultured in 6-well plates ($1–2 \times 10^6$ cells/well) were treated with MEM, 0.1 nM ADM, 1 nM ADM, or 10 nM ADM for 300 s (5 min). In time course experiments, the cells were incubated with 10 nM ADM for 0, 50, 100, and 300 s. To determine the mechanisms of the ADM-induced nNOS dephosphorylation, the cells were pretreated with MEM, 0.1 μM OA, 1 μM FK506, 0.1 μM CsA, 50 μM BAPTA-AM, or 5 μM H-89 for 10 min, followed by 5-min treatment with MEM or 10 nM ADM in the absence or present of respective blockers.

The cells were harvested with lysis buffer supplemented with 1:100 phosphatase inhibitor cocktail 1 (Sigma-Aldrich). Proteins in homogenates were separated by electrophoresis on 8% SDS-polyacrylamide gels and transferred to nitrocellulose membranes. The membranes were probed with 1:200 rabbit anti-phospho-$nNOS^{Ser847}$ antibody (Santa Cruz), and expression of phosphorylated $nNOS^{Ser847}$ was detected with chemiluminescence reagents (PerkinElmer Life and Analytical Sciences, Waltham, MA) and quantified with Quantity One 4.3.1 (Bio-Rad Laboratories, Hercules, CA). Because of some variability in densities of individual bands along their widths, rectangles of the same size were drawn to entirely include each band, and the mean densities within these areas were measured to indicate expression levels of $nNOS^{Ser\ 847}$. The same membranes were stripped and probed with 1:500 rabbit anti-nNOS antibody (Santa Cruz) or 1:4000 mouse anti-β-actin antibody (Sigma-Aldrich), and densities of total nNOS and β-actin bands were measured as described above. The levels of nNOS were calculated as the ratio of nNOS/β-actin and normalized to results in MEM treatment, whereas the levels of phosphorylated $nNOS^{Ser\ 847}$ are presented as the ratio of phospho-$nNOS^{ser847}$/nNOS and normalized to results in MEM treatment.

Statistical Analysis. Data were presented as mean values ± S.E.M. Statistical analyses were carried out with SigmaStat software. Depending on the experiments, differences among groups were determined by one-way or two-way analysis of variance analysis, followed by the post hoc Student-Newman-Keuls test when the analysis of variance analysis indicated significant differences. $P < 0.05$ indicated statistical significance.

Results

Expression of CRLR, RAMP-2/3, and nNOS in Hypothalamic Neurons. Using double-labeling immunocytochemistry, we found that approximately 20% of cells in the cultures coexpressed the ADM receptor components CRLR and RAMP-2/RAMP-3 (Fig. 1, A and B). In addition, colocalization of CRLR with RAMP-2/RAMP-3 was found in the soma, neurites, and, more importantly, cell membrane, which suggests that functional ADM receptors are present in these cells.

The majority of CRLR-positive cells also expressed nNOS (Fig. 1C), indicating that these putative ADM-responsive cells have the ability to produce NO. We also found that a proportion of nNOS was colocalized with CRLR on the membrane. Because similar colocalization of nNOS and the *N*-methyl-D-aspartate (NMDA) receptor has been considered to ensure rapid nNOS activation after NMDA stimulation (Aoki et al., 1997), the observed proximity of nNOS and ADM receptor may also provide the morphological basis for the functional interaction between ADM and nNOS.

ADM Increases $[Ca^{2+}]_i$ and NO Production in Receptor- and nNOS-Dependent Manners. Using fluorescence live-cell imaging, the relative levels of $[Ca^{2+}]_i$ and NO production were represented as fluorescence intensities generated by Calcium Orange and DAF-FM, respectively. Of the 523 cells that were studied, 102 cells (19.5%) responded to ADM with increased NO production. Results described below were obtained from these ADM-responsive neurons.

Figure 2A shows that in 10 ADM-responsive cells, treatment with 10 nM ADM (5 min) induced a rapid and transient increase in $[Ca^{2+}]_i$ with a maximal increase of 164 ± 11% (versus the basal level) occurring 50 s after the initiation of the treatment. This response then gradually decreased and finally dissipated when ADM was washed away with MEM. The subsequent treatment with 1 nM ADM (5 min) led to a smaller increase (138 ± 11%). At the same time, 10 nM ADM (5 min) elicited a sustained increase in NO production with a maximal increase of 177 ± 13%, whereas 1 nM ADM (5 min) evoked a similar but smaller increase (143 ± 15%). Figure 2B shows that in nine cells, the first treatment with 1 nM ADM (5 min) increased $[Ca^{2+}]_i$ and NO production to 138 ± 10 and 146 ± 3%, respectively, and the subsequent treatment with 10 nM ADM (5 min) induced larger responses in $[Ca^{2+}]_i$ and

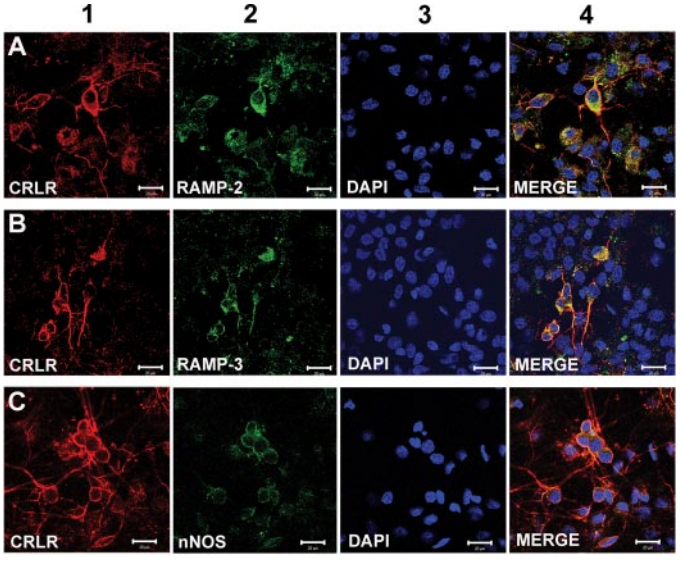

Fig. 1. Confocal images of hypothalamic neurons double-labeled for CRLR and RAMP-2 (A), RAMP-3 (B), or nNOS (C). CRLR-positive cells are identified by cy3 (red) fluorescence in 1; RAMPs or nNOS immunoreactivity is localized by Alexa 488 (green) fluorescence in 2; the presence of cells is indicated by nuclear 4′-6-diamidino-2-phenylindole (blue) staining in 3; and colocalization of CRLR with RAMPs or nNOS is illustrated by the yellow color in the merge images in 4. Scale bars, 20 μM.

NO production (174 ± 13 and 173 ± 17%, respectively). These results demonstrate that ADM simultaneously stimulates increased $[Ca^{2+}]_i$ and NO production in hypothalamic neurons and that the effects of ADM were repeatable and concentration-related. In control experiments, transient and small (less than 20%) decreases in Calcium Orange-generated fluorescence were observed when MEM was injected into the chamber at the corresponding time points, whereas DAF-FM-generated fluorescence gradually decreased over time by no more than 16% of the basal levels (Fig. 2C), presumably caused by photobleaching.

In eight cells that responded to ADM (10 nM, 5 min) with increased $[Ca^{2+}]_i$ and NO production, a second treatment with the same concentration of ADM elicited significantly attenuated Ca^{2+} or NO responses in the presence of ADM_{22-52} (10 nM, 10 min) (Fig. 3A). On the other hand, the ADM-induced increases in $[Ca^{2+}]_i$ and NO production in five cells were not affected by $CGRP_{8-37}$ (Fig. 3B). Because the ADM receptor, composed of CRLR and RAMP-2, is more sensitive to ADM_{22-52}, whereas the CRLR-RAMP-3 receptor complex shows a clear preference for $CGRP_{8-37}$-induced antagonism (Hay et al., 2004), these results suggest that the CRLR-RAMP-2 receptor complex plays the predominant role in mediating ADM's effects in the hypothalamic neurons.

In seven cells, ADM-stimulated NO production was completely blocked with the selective nNOS inhibitor vinyl-L-NIO (2 μM) (Fig. 4A), demonstrating that activation of nNOS is responsible for the ADM-stimulated NO production. Vinyl-L-NIO itself decreased resting levels of NO production to 48 ± 10%, which suggests that basal NO production in the hypothalamic neurons is also dependent on activity of nNOS. The ADM-induced increase in $[Ca^{2+}]_i$ was not affected by vinyl-L-NIO.

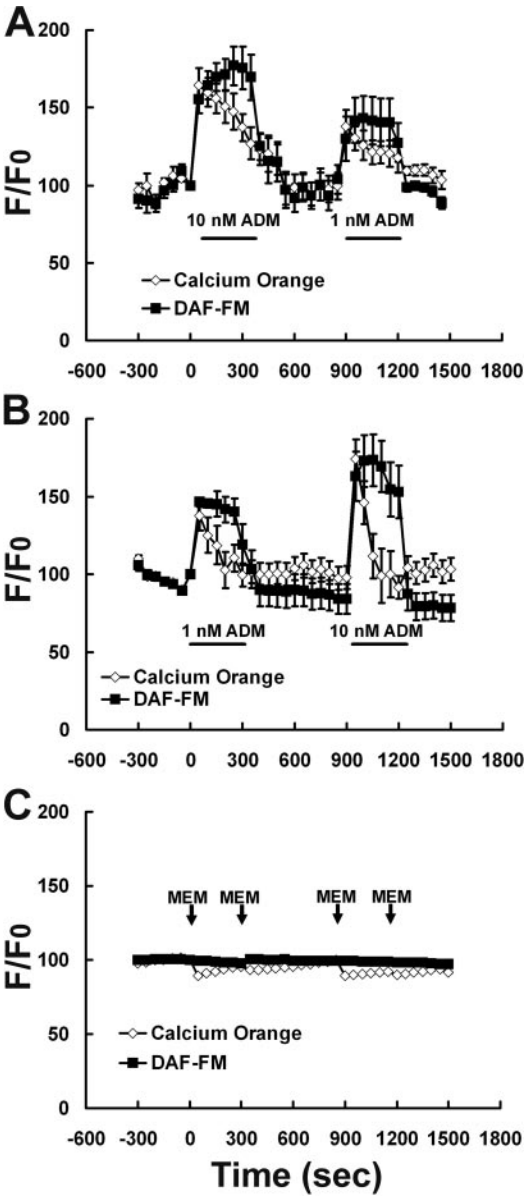

Fig. 2. Effects of ADM on $[Ca^{2+}]_i$ and NO production in hypothalamic neurons. A, relative changes in Calcium Orange- and DAF-FM-generated fluorescence intensities in 10 cells that were treated with ADM (10 nM, 5 min), washed with MEM (10 min), and then treated with ADM (1 nM, 5 min). B, relative changes in Calcium Orange- and DAF-FM-generated fluorescence intensities in nine cells that were treated with ADM (1 nM, 5 min), washed with MEM (10 min), and then treated with ADM (10 nM, 5 min). C, relative changes in Calcium Orange- and DAF-FM-generated fluorescence intensities in seven cells that were treated with MEM at indicated time points. Values are mean ± S.E.M.

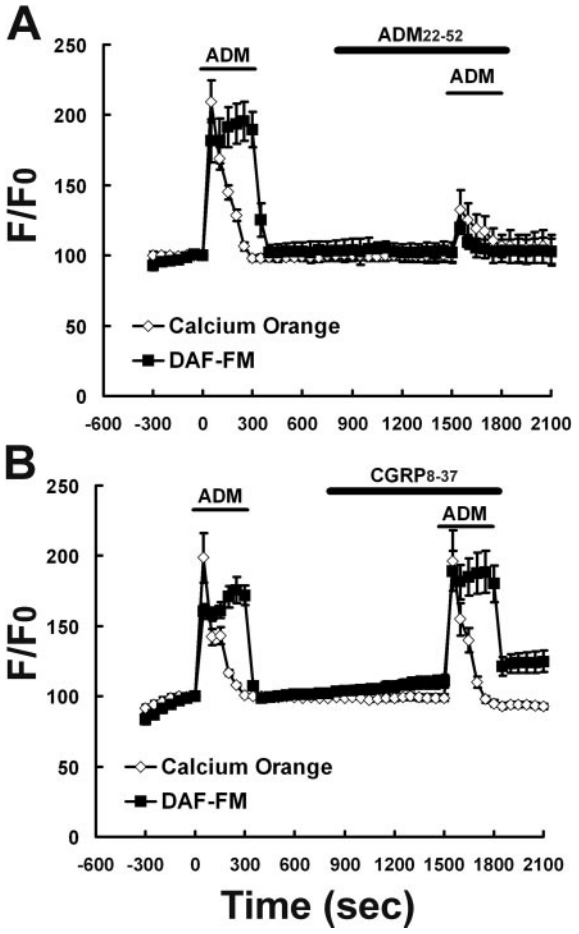

Fig. 3. Effects of ADM_{22-52} and $CGRP_{8-37}$ on the ADM-induced responses in $[Ca^{2+}]_i$ and NO production in hypothalamic neurons. A, relative changes in Calcium Orange- and DAF-FM-generated fluorescence intensities in eight cells that were treated with ADM (10 nM, 5 min), washed with MEM (10 min), and then treated with ADM_{22-52} (10 nM, 10 min) followed by ADM plus ADM_{22-52} (5 min). B, relative changes in Calcium Orange- and DAF-FM-generated fluorescence intensities in five cells that were treated with ADM (10 nM, 5 min), washed with MEM (10 min), and then treated with $CGRP_{8-37}$ (10 nM, 10 min) followed by ADM plus $CGRP_{8-37}$ (5 min). Values are mean ± S.E.M.

Elevation of $[Ca^{2+}]_i$ Is Required for ADM-Stimulated NO Production. Because ADM simultaneously elevates $[Ca^{2+}]_i$ and NO production, we used BAPTA-AM (50 μM) to determine whether ADM-induced NO production is Ca^{2+}-dependent. Figure 4B shows that in 10 cells, the pretreatment with BAPTA-AM (10 min) abolished the ADM-stimulated NO production. These results indicate that increased $[Ca^{2+}]_i$ is required for the ADM-induced NO production. BAPTA-AM itself reduced the resting levels of $[Ca^{2+}]_i$ and NO production to approximately 33 ± 8 and 38 ± 12% (Fig. 4B), respectively, suggesting that basal NO production in these cells is also a Ca^{2+}-dependent event.

The cAMP-PKA Pathway Mediates ADM-Stimulated Ca^{2+} and NO Responses. To determine whether ADM stimulates increases in $[Ca^{2+}]_i$ and NO production via the cAMP-PKA pathway, we first evaluated the effects of ADM on cAMP levels. Figure 5A shows that treatment with ADM at 1 or 10 nM for 5 min significantly increased intracellular cAMP levels compared with controls (vehicle treatment) and that the effect of 10 nM ADM was significantly higher than that of 1 nM ADM. To provide further evidence that the cAMP-PKA pathway mediates the ADM-stimulated increases in $[Ca^{2+}]_i$ and NO production, we assessed these ADM-induced responses after the cells were pretreated with the PKA inhibitors H-89 (5 μM) or Rp-cAMP (50 μM). Increases in $[Ca^{2+}]_i$ and NO production evoked by ADM (10 nM, 5 min) were abolished by 10-min pretreatment with 5 μM H-89 (26 cells) (Fig. 5B) or with 50 μM Rp-cAMP (7 cells) (Fig. 5C). Note that H-89 itself increased the basal levels of $[Ca^{2+}]_i$ to 149 ± 16% (Fig. 5B).

nNOS Dephosphorylation Contributes to ADM-Stimulated NO Production. Because phosphorylation of nNOS

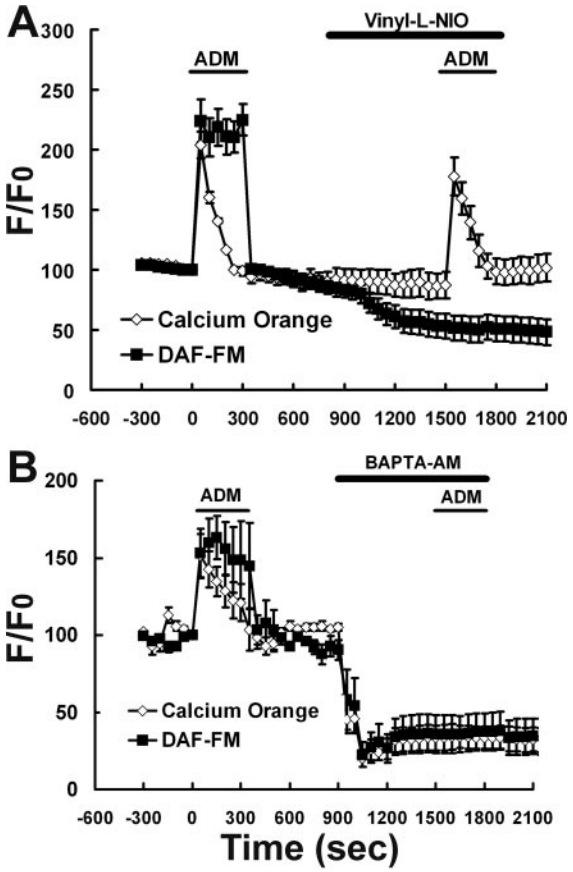

Fig. 4. Effects of vinyl-L-NIO and BAPTA-AM on the ADM-induced responses in $[Ca^{2+}]_i$ and NO production in hypothalamic neurons. A, relative changes in Calcium Orange- and DAF-FM-generated fluorescence intensities in seven cells that were treated with ADM (10 nM, 5 min), washed with MEM (10 min), and then treated with vinyl-L-NIO (2 μM, 10 min) followed by ADM plus vinyl-L-NIO (5 min). B, relative changes in Calcium Orange- and DAF-FM-generated fluorescence intensities in 10 cells that were treated with ADM (10 nM, 5 min), washed with MEM (10 min), and then treated with BAPTA-AM (50 μM, 10 min) followed by ADM plus BAPTA-AM (5 min). Values are mean ± S.E.M.

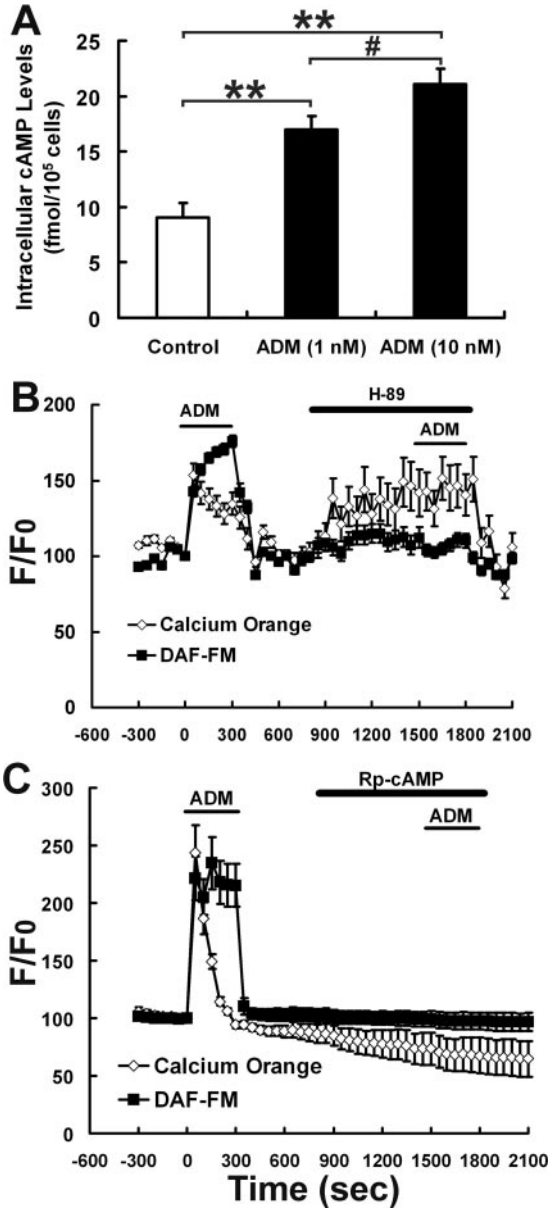

Fig. 5. A, effects of ADM on intracellular cAMP levels in hypothalamic neurons. Intracellular cAMP levels were measured after hypothalamic neurons were treated with vehicle, 1 nM ADM or 10 nM ADM for 5 min; n = 8 in each group. Values are mean ± S.E.M. **, $P < 0.01$ versus control; #, $P < 0.05$ versus 1 nM ADM treatment. B and C, effects of PKA inhibitors on the ADM-induced responses in $[Ca^{2+}]_i$ and NO production in hypothalamic neurons. B, relative changes in Calcium Orange- and DAF-FM-generated fluorescence intensities in 26 cells that were treated with ADM (10 nM, 5 min), washed with MEM (10 min), and then treated with H-89 (5 μM, 10 min) followed by ADM plus H-89 (5 min). C, relative changes in Calcium Orange- and DAF-FM-generated fluorescence intensities in seven cells that were treated with ADM (10 nM, 5 min), washed with MEM (10 min), and then treated with Rp-cAMP (50 μM, 10 min) followed by ADM plus Rp-cAMP (5 min). Values are mean ± S.E.M.

at serine 847 has been shown to exert an inhibitory effect on the activity of nNOS (Komeima et al., 2000), we investigated whether ADM modulates this phosphorylation. ADM application (10 nM, 5 min) significantly decreased nNOS phosphorylation at serine 847 by 57 ± 14%, whereas total nNOS levels remained unchanged (Fig. 6, A and B). Lower doses of ADM (0.1 and 1 nM, 5 min) also seemed to dephosphorylate nNOS, but these responses were not statistically significant (Fig. 6, A and B). Finally, ADM induced nNOS dephosphorylation in a time-dependent manner so that 10 nM ADM significantly decreased nNOS phosphorylation by 38 ± 14 and 57 ± 13% at 100 and 300 s, respectively, whereas 50 s after ADM treatment, the phosphorylation levels of nNOS were comparable with the basal levels (Fig. 6, C and D).

PP1/PP2A and calcineurin have been shown to mediate NMDA-induced nNOS dephosphorylation at serine 847 in cortical neurons (Rameau et al., 2003). Therefore, we asked whether PP1/PP2A and calcineurin are responsible for the ADM-induced nNOS dephosphorylation. Pretreatment with OA (0.1 μM, 10 min), a PP1/PP2A inhibitor, abrogated the decrease in nNOS phosphorylation induced by ADM (10 nM, 5 min). Similar inhibition of nNOS dephosphorylation was observed when the cells were pretreated with calcineurin inhibitors FK506 (1 μM, 10 min) or CsA (0.1 μM, 10 min) (Fig. 7, A and B). Thus, these data indicate that both PP1/PP2A and calcineurin are recruited by ADM to dephosphorylate nNOS.

To determine whether Ca^{2+} signaling and/or the cAMP-PKA pathway are involved in ADM's effect on nNOS phosphorylation, we assessed ADM-induced nNOS dephosphorylation after the cells were pretreated with MEM, BAPTA-AM, or H-89. Although ADM (10 nM, 5 min) seemed to decrease nNOS dephosphorylation in the presence of BAPTA-AM (50 μM), this decrease was not statistically significant (ADM plus BAPTA-AM, 37 ± 8%, versus BAPTA-AM, 61 ± 8%, $P = 0.066$) (Fig. 7, C and D). Thus, Ca^{2+} signaling seems to be at least partly responsible for ADM-induced nNOS dephosphorylation. Pretreatment with H-89 (5 μM, 10 min) abolished ADM-induced nNOS dephosphorylation (Fig. 7, C and D), indicating that the PKA-associated pathway is required for the ADM-induced nNOS dephosphorylation. BAPTA-AM and H-89 alone also significantly decreased the basal phosphorylation levels of nNOS to 61 ± 8 and 44 ± 10%, respectively (Fig. 7, C and D).

Finally, we investigated whether nNOS dephosphorylation contributes to ADM-induced NO production. Figure 8A shows that in eight cells, pretreatment with OA (0.1 μM, 10 min) significantly attenuated the amplitude of the ADM-induced increases in NO production from 87 ± 15 to 40 ± 13%, whereas responses in $[Ca^{2+}]_i$ to ADM treatment were not affected. Likewise, the calcineurin inhibitors FK506 (1 μM, 10 min) or CsA (0.1 μM, 10 min) significantly reduced the amplitude of the ADM-induced increases in NO production from 54 ± 16 to 21 ± 16% (in six cells) or from to 81 ± 11 to 19 ± 8% (in six cells), respectively (Fig. 8, B and C). These results show that PP1/PP2A and calcineurin are involved in the ADM-induced NO production. Treatments with OA, FK506, or CsA alone decreased the basal NO production levels to 68 ± 10, 84 ± 10, or 75 ± 5%, respectively, suggesting that PP1/PP2A and calcineurin also contribute to the maintenance of basal nNOS activity in hypothalamic neurons.

Discussion

We demonstrate in this study that ADM rapidly stimulates an increase in NO production in cultured hypothalamic neurons and that this effect occurs in a Ca^{2+}-dependent manner. In addition, we suggest that nNOS dephosphorylation by protein phosphatases mediates ADM-stimulated increases in NO production. Finally, our data show that the cAMP-PKA pathway mediates the NO response by regulating intracellular Ca^{2+} dynamics and nNOS phosphorylation.

In vivo evidence suggests that ADM stimulates NO production in neurons. For example, the ADM receptor component RAMP-2 is expressed in nNOS-positive neurons (Xu and Krukoff, 2004b), and peripheral or central administration of

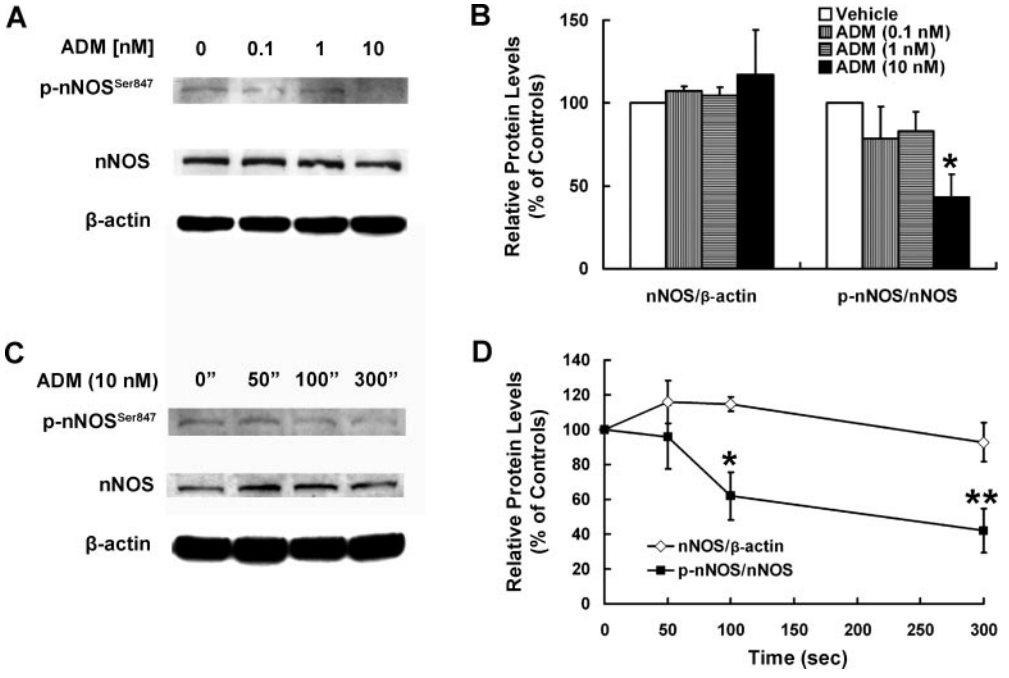

Fig. 6. Effects of ADM on serine 847 phosphorylation of nNOS. A and B, hypothalamic neurons were treated with vehicle or 0.1 to 10 nM ADM for 5 min. C and D, hypothalamic neurons were treated with 10 nM ADM for 0, 50, 100, or 300 s. Protein samples were probed with anti-phospho-nNOS^{ser847}, anti-nNOS, and anti-β-actin antibodies. Representative photographs of Western blotting results are shown in A and C; relative nNOS and phospho-nNOS^{ser847} levels are presented in B and D as the ratios of nNOS/β-actin and phospho-nNOS^{ser847}/nNOS, respectively. Values are mean ± S.E.M.; $n = 3$ (B) and $n = 4$ (D). *, $P < 0.05$, and **, $P < 0.01$, versus the controls.

ADM activates nNOS-positive neurons in the brain (Shan and Krukoff, 2000; Shan and Krukoff, 2001). Consistent with these findings, we now show that ADM stimulates a rapid and nNOS-mediated NO synthesis in cultured primary neurons in a receptor-dependent manner. Increased NO synthesis in neurons is important for the physiological actions of ADM in the brain because central NO mediates ADM's effects on blood pressure regulation, demonstrated by our previous observations that alterations in blood pressure and heart rate induced by ADM in the PVN or rostral ventrolateral medulla are attenuated or abolished by NOS inhibitors (Xu and Krukoff, 2004a,b). Increased NO production may also play a role in the regulatory effects of ADM on hypothalamic vasopressin secretion and body fluid homeostasis (Taylor et al., 2005). Supporting this suggestion, intracerebroventricular ADM administration activates nNOS-positive neurons in the magnocellular subdivision of the PVN (Shan and Krukoff, 2001), where vasopressin is produced. In addition, ADM has been shown to protect neurons from ischemia, and this effect is associated with elevated NO levels (Xia et al., 2006).

In an attempt to identify mechanisms by which ADM activates nNOS and stimulates NO production, we investigated the involvement of three distinct but related signaling pathways: protein phosphatases, Ca^{2+} signaling, and the cAMP-PKA pathway. First, ADM is shown to concentration- and time-dependently induce dephosphorylation of nNOS at serine 847 via activities of PP1/PP2A and calcineurin. Our finding that inhibition of these phosphatases significantly attenuates NO synthesis suggests that this nNOS dephosphorylation contributes to ADM-induced NO production. The role of these phosphatases to mediate NMDA-induced nNOS dephosphorylation at serine 847 and elevated NO production has also been demonstrated in rat cortical neurons (Rameau et al., 2003).

It has been well-established that elevations in $[Ca^{2+}]_i$ lead to activation of nNOS by inducing the interaction of CaM and nNOS (Panda et al., 2001). We confirm that an increase in $[Ca^{2+}]_i$ is required for the ADM-stimulated NO production in hypothalamic neurons because ADM simultaneously increases $[Ca^{2+}]_i$ and NO production, and ADM-stimulated NO production is abolished when cytosolic free Ca^{2+} is chelated with BAPTA-AM. We found that the ADM-induced Ca^{2+} increase dissipates rapidly, whereas the NO response is sustained, suggesting that, although a transient elevation in $[Ca^{2+}]_i$ is necessary for the initial activation of nNOS, the maintenance of nNOS activity may be Ca^{2+}-independent. In support of this idea, it has been shown in vitro that a transient increase in $[Ca^{2+}]_i$ in endothelial cells is associated with a sustained interaction of CaM and endothelial NOS, another Ca^{2+}-CaM-dependent isoform of NOS (Jobin et al., 2003).

Besides facilitating the interaction of CaM and nNOS, concentrated Ca^{2+} may also activate nNOS, at least in part, by dephosphorylating the enzyme, based on the observation that chelation of cytosolic-free Ca^{2+} blunts ADM-induced nNOS dephosphorylation. ADM-stimulated Ca^{2+} accumulation probably leads to activation of calcineurin (Shou et al., 2004), which, in turn, dephosphorylates nNOS. It is interesting that we also found that application of BAPTA-AM alone significantly decreases nNOS phosphorylation in the resting state. We believe that this response can be attributed to the inhibition of CaMKII evoked by Ca^{2+} chelation, given that CaMKII is involved in the constitutive phosphorylation of nNOS (Komeima et al., 2000).

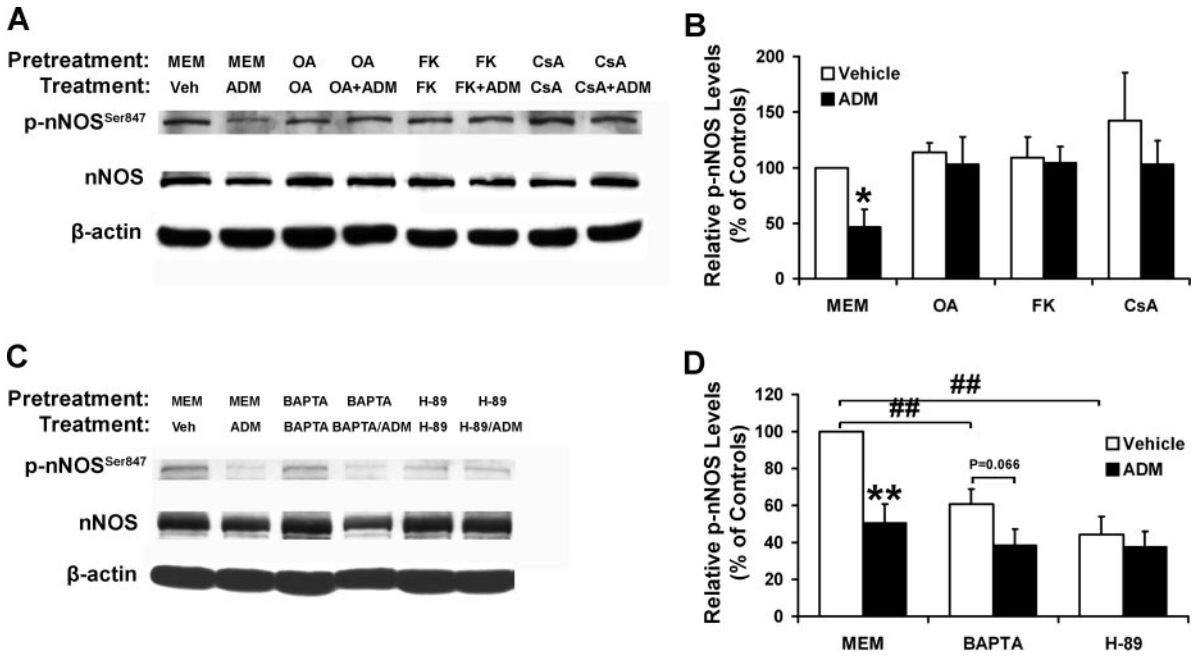

Fig. 7. Effects of protein phosphatase inhibitors, BAPTA-AM and H-89, on ADM-induced nNOS dephosphorylation. A and B, hypothalamic neurons were pretreated with MEM, OA (0.1 μM), FK506 (1 μM), or CsA (0.1 μM) for 10 min followed by 5-min treatment with vehicle or ADM (10 nM) in the absence or presence of respective inhibitors. C and D, hypothalamic neurons were pretreated with MEM, BAPTA-AM (50 μM), or H-89 (5 μM) for 10 min followed by 5-min treatment with vehicle or ADM (10 nM) in the absence or presence of respective inhibitors. Protein samples were probed with anti-phospho-nNOS^{ser847}, anti-nNOS, and anti-β-actin antibodies. Representative photographs of Western blotting results are shown in A and C; relative phospho-nNOS^{ser847} levels are presented in B and D as the ratio of phospho-nNOS^{ser847}/nNOS. Values are mean ± S.E.M.; $n = 4$ (B) and $n = 6$ (D). *, $P < 0.05$, and **, $P < 0.01$, ADM treatment versus the vehicle treatment; $P = 0.066$ BAPTA-AM versus BAPTA-AM plus ADM; ##, $P < 0.01$ BAPTA-AM or H-89 pretreatment versus MEM pretreatment.

The cAMP-PKA pathway is coupled to ADM receptors in various types of cells (Kitamura et al., 1993; Shimekake et al., 1995), including neural cells (Xu and Krukoff, 2005). In addition, PKA mediates nNOS activation induced by diverse stimuli, such as electrical field stimulation (Ferrer et al., 2004) and application of endothelin (Jaureguiberry et al., 2004) or β-adrenoceptor agonists (Birder et al., 2002). We now show that ADM increases cAMP levels in hypothalamic neurons and that the cAMP-PKA pathway mediates the ADM-induced NO production, demonstrated by the blockade of NO responses in the presence of the PKA inhibitors H-89 and Rp-cAMP.

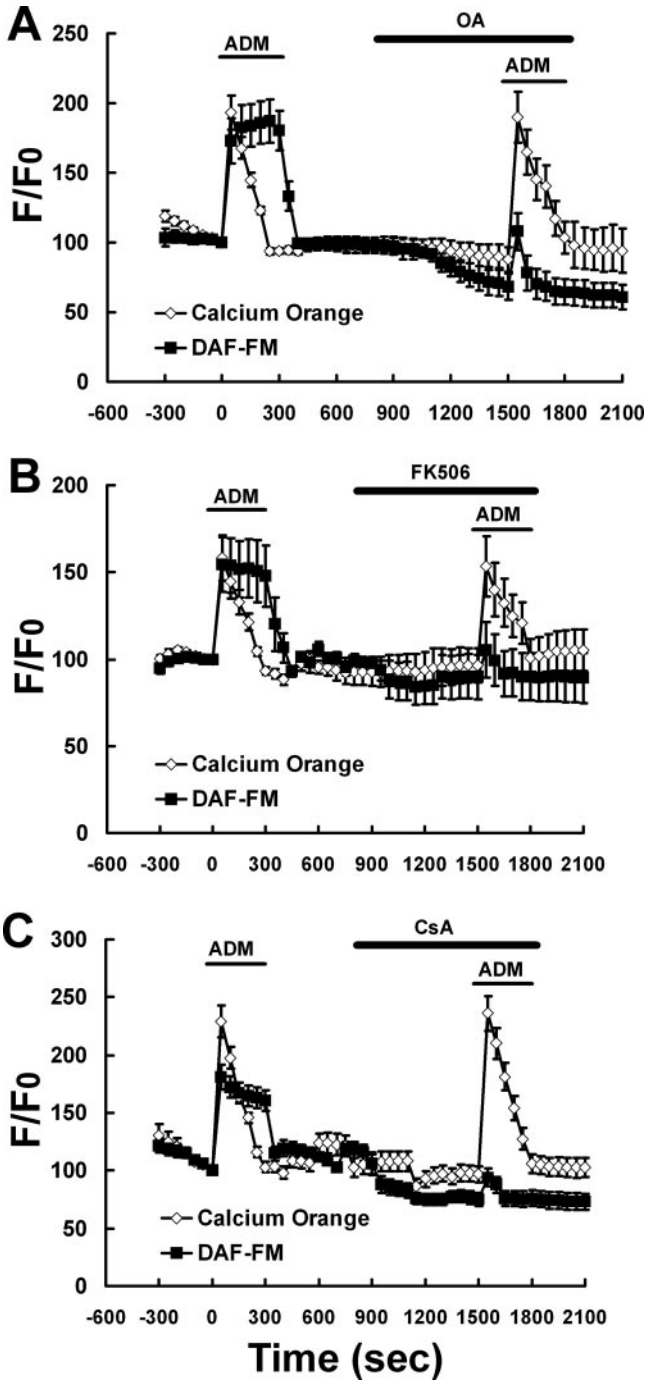

Fig. 8. Effects of protein phosphatase inhibitors on the ADM-induced responses in $[Ca^{2+}]_i$ and NO production in hypothalamic neurons. A, relative changes in Calcium Orange- and DAF-FM-generated fluorescence intensities in eight cells that were treated with ADM (10 nM, 5 min), washed with MEM (10 min), and then treated with OA (0.1 μM, 10 min) followed by ADM plus OA (5 min). B, relative changes in Calcium Orange- and DAF-FM-generated fluorescence intensities in six cells that were treated with ADM (10 nM, 5 min), washed with MEM (10 min), and then treated with FK506 (1 μM, 10 min) followed by ADM plus FK506 (5 min). C, relative changes in Calcium Orange- and DAF-FM-generated fluorescence intensities in six cells that were treated with ADM (10 nM, 5 min), washed with MEM (10 min), and then treated with CsA (0.1 μM, 10 min) followed by ADM plus H-89 (5 min). Values are mean ± S.E.M.

Two potential cascades may be activated by the cAMP-PKA pathway to mediate ADM's effects. First, the elimination of ADM-stimulated increases in $[Ca^{2+}]_i$ with H-89 or Rp-cAMP suggests that PKA mediates ADM-stimulated NO production by stimulating accumulation of intracellular Ca^{2+}. Likewise, this PKA-Ca^{2+}-NO cascade has been reported in urothelial cells (Birder et al., 2002), enterocytes (Canani et al., 2003), and neuroblastoma cells (Xu and Krukoff, 2005). Alternatively but not exclusively, PKA may stimulate nNOS activation by activating protein phosphatases to remove the inhibitory serine 847 phosphorylation from nNOS. The involvement of the PKA-phosphatase-NO cascade is supported by the observation that H-89 abolishes the ADM-induced nNOS dephosphorylation. PKA may activate phosphatases through multiple signal cascades. For example, PKA may indirectly activate PP1, because PKA has been shown to suppress activities of endogenous PP1 inhibitors such as the nuclear inhibitor of PP1 (Beullens et al., 1993) and gastrointestinal- and brain-specific PP1-inhibitory protein (Liu et al., 2004). PKA may also activate calcineurin via a Ca^{2+}-dependent mechanism given that PKA stimulates intracellular accumulation of Ca^{2+}, as discussed above.

The PKA inhibitor H-89 seems to increase $[Ca^{2+}]_i$ in hypothalamic neurons. This response is probably caused by the nonspecific effects of H-89 rather than its anti-PKA property because another PKA inhibitor, Rp-cAMP, has no effect on basal $[Ca^{2+}]_i$. Indeed, H-89-stimulated Ca^{2+} accumulation has been reported to occur in muscle cells (Lahouratate et al., 1997), lymphocytes (de la Rosa et al., 2001), and neuroblastoma cells (Xu and Krukoff, 2005) and is presumably caused by nonspecific effects of H-89 on the endoplasmic reticulum-associated Ca^{2+} ATPase (de la Rosa et al., 2001).

H-89 itself also decreases nNOS phosphorylation in the resting state, consistent with previous studies suggesting that PKA contributes to the constitutive phosphorylation of nNOS (Bredt et al., 1992; Dinerman et al., 1994). It is intriguing, however, that H-89 alone induces both an increase in $[Ca^{2+}]_i$ and a decrease in nNOS phosphorylation and that these processes are not accompanied by increased NO production. We interpret these results to suggest that nonspecific H-89-induced intracellular Ca^{2+} accumulation occurs at a site distant from nNOS so that the increase in $[Ca^{2+}]_i$ is not sufficient to activate nNOS. In fact, it has been suggested that the proximity of nNOS and Ca^{2+} is essential for activation of the enzyme (Kone et al., 2003). On the other hand, these data may also suggest that elevations in $[Ca^{2+}]_i$ and nNOS dephosphorylation are required but not sufficient to induce nNOS activation and NO production and that other unknown PKA-dependent mechanisms are required for these processes. For instance, it has been demonstrated that NOS-interaction protein (NOSIP) interacts with and inhibits nNOS (Dreyer et al., 2004). The fact that NOSIP contains the consensus sequence for PKA supports the idea that PKA may

contribute to the regulation of nNOS partly through its actions on NOSIP.

In summary, we have demonstrated that ADM stimulates NO production from hypothalamic neurons, and our data suggest that multiple mechanisms are involved in this effect. Thus, binding of ADM to the CRLR-RAMP-2 receptor complex stimulates accumulation of intracellular Ca^{2+} via PKA-mediated mechanisms. Elevation in $[Ca^{2+}]_i$ leads to formation of the Ca^{2+}-CaM complex, which, in turn, binds to nNOS. PKA/Ca^{2+}-associated pathways lead to PP1/PP2A- and calcineurin-mediated dephosphorylation of nNOS. According to our model, both of these processes may finally contribute to activation of nNOS and production of NO. These data not only provide important in vitro evidence supporting the notion that NO mediates at least some of ADM's actions in the brain, they also contribute to the fundamental understanding of ADM-initiated signaling in neurons.

References

Aoki C, Rhee J, Lubin M, and Dawson TM (1997) NMDA-R1 subunit of the cerebral cortex co-localizes with neuronal nitric oxide synthase at pre- and postsynaptic sites and in spines. *Brain Res* **750:**25–40.

Beullens M, Van Eynde A, Bollen M, and Stalmans W (1993) Inactivation of nuclear inhibitory polypeptides of protein phosphatase-1 (NIPP-1) by protein kinase A. *J Biol Chem* **268:**13172–13177.

Birder LA, Nealen ML, Kiss S, de Groat WC, Caterina MJ, Wang E, Apodaca G, and Kanai AJ (2002) Beta-adrenoceptor agonists stimulate endothelial nitric oxide synthase in rat urinary bladder urothelial cells. *J Neurosci* **22:**8063–8070.

Boyadjieva NI, Chen CP, and Sarkar DK (2003) Role of nitric oxide in alcohol alteration of beta-endorphin release from hypothalamic cells in primary cultures. *Alcohol Clin Exp Res* **27:**1813–1818.

Bredt DS, Ferris CD, and Snyder SH (1992) Nitric oxide synthase regulatory sites. Phosphorylation by cyclic AMP-dependent protein kinase, protein kinase C, and calcium/calmodulin protein kinase; identification of flavin and calmodulin binding sites. *J Biol Chem* **267:**10976–10981.

Canani RB, Cirillo P, Buccigrossi V, De Marco G, Mallardo G, Bruzzese E, Polito G, and Guarino A (2003) Nitric oxide produced by the enterocyte is involved in the cellular regulation of ion transport. *Pediatr Res* **54:**64–68.

de la Rosa LA, Vilarino N, Vieytes MR, and Botana LM (2001) Modulation of thapsigargin-induced calcium mobilisation by cyclic AMP-elevating agents in human lymphocytes is insensitive to the action of the protein kinase A inhibitor H-89. *Cell Signal* **13:**441–449.

Dinerman JL, Steiner JP, Dawson TM, Dawson V, and Snyder SH (1994) Cyclic nucleotide dependent phosphorylation of neuronal nitric oxide synthase inhibits catalytic activity. *Neuropharmacology* **33:**1245–1251.

Dong Y and White FJ (2003) Dopamine D1-class receptors selectively modulate a slowly inactivating potassium current in rat medial prefrontal cortex pyramidal neurons. *J Neurosci* **23:**2686–2695.

Dreyer J, Schleicher M, Tappe A, Schilling K, Kuner T, Kusumawidijaja G, Muller-Esterl W, Oess S, and Kuner R. (2004) Nitric oxide synthase (NOS)-interacting protein interacts with neuronal NOS and regulates its distribution and activity. *J Neurosci* **24:**10454–10465.

Ferrer M, Sanchez M, Martin Mdel C, Marquez-Rodas I, Alonso MJ, Salaices M, and Balfagon G (2004) Protein kinase A increases electrical stimulation-induced neuronal nitric oxide release in rat mes enteric artery. *Eur J Pharmacol* **487:**167–173.

Hay DL, Conner AC, Howitt SG, Smith DM, and Poyner DR (2004) The pharmacology of adrenomedullin receptors and their relationship to CGRP receptors. *J Mol Neurosci* **22:**105–114.

Ishimitsu T, Ono H, Minami J, and Matsuoka H (2006) Pathophysiologic and therapeutic implications of adrenomedullin in cardiovascular disorders. *Pharmacol Ther* **111:**909–927.

Jaureguiberry MS, di Nunzio AS, Dattilo MA, Bianciotti LG, and Vatta MS (2004) Endothelin 1 and 3 enhance neuronal nitric oxide synthase activity through ETB receptors involving multiple signaling pathways in the rat anterior hypothalamus. *Peptides* **25:**1133–1138.

Jobin CM, Chen H, Lin AJ, Yacono PW, Igarashi J, Michel T, and Golan DE (2003) Receptor-regulated dynamic interaction between endothelial nitric oxide synthase and calmodulin revealed by fluorescence resonance energy transfer in living cells. *Biochemistry* **42:**11716–11725.

Kitamura K, Kangawa K, Kawamoto M, Ichiki Y, Nakamura S, Matsuo H, and Eto T (1993) Adrenomedullin: a novel hypotensive peptide isolated from human pheochromocytoma. *Biochem Biophys Res Commun* **192:**553–560.

Komeima K, Hayashi Y, Naito Y, and Watanabe Y (2000) Inhibition of neuronal nitric-oxide synthase by calcium/calmodulin-dependent protein kinase IIα through Ser847 phosphorylation in NG108-15 neuronal cells. *J Biol Chem* **275:**28139–28143.

Kone BC, Kuncewicz T, Zhang W, and Yu ZY (2003) Protein interactions with nitric oxide synthases: controlling the right time, the right place, and the right amount of nitric oxide. *Am J Physiol Renal Physiol* **285:**F178–F190.

Krukoff TL (1999) Central actions of nitric oxide in regulation of autonomic functions. *Brain Res Brain Res Rev* **30:**52–65.

Lahouratate P, Guibert J, Camelin JC, and Bertrand I (1997) Specific inhibition of cardiac and skeletal muscle sarcoplasmic reticulum Ca^{2+} pumps by H-89. *Biochem Pharmacol* **54:**991–998.

Liu QR, Zhang PW, Lin Z, Li QF, Woods AS, Troncoso J, and Uhl GR (2004) GBPI, a novel gastrointestinal- and brain-specific PP1-inhibitory protein, is activated by PKC and inactivated by PKA. *Biochem J* **377:**171–181.

McLatchie LM, Fraser NJ, Main MJ, Wise A, Brown J, Thompson N, Solari R, Lee MG, and Foord SM (1998) RAMPs regulate the transport and ligand specificity of the calcitonin-receptor-like receptor. *Nature* **393:**333–339.

Panda K, Ghosh S, and Stuehr DJ (2001) Calmodulin activates intersubunit electron transfer in the neuronal nitric-oxide synthase dimer. *J Biol Chem* **276:**23349–23356.

Prendergast MA, Harris BR, Mullholland PJ, Blanchard JA 2nd, Gibson DA, Holley RC, and Littleton JM (2004) Hippocampal CA1 region neurodegeneration produced by ethanol withdrawal requires activation of intrinsic polysynaptic hippocampal pathways and function of *N*-methyl-D-aspartate receptors. *Neuroscience* **124:**869–877.

Rameau GA, Chiu LY, and Ziff EB (2003) NMDA receptor regulation of nNOS phosphorylation and induction of neuron death. *Neurobiol Aging* **24:**1123–1133.

Shan J and Krukoff TL (2000) Area postrema ablation attenuates activation of neurones in the paraventricular nucleus in response to systemic adrenomedullin. *J Neuroendocrinol* **12:**802–810.

Shan J and Krukoff TL (2001) Intracerebroventricular adrenomedullin stimulates the hypothalamo-pituitary-adrenal axis, the sympathetic nervous system and production of hypothalamic nitric oxide. *J Neuroendocrinol* **13:**975–984.

Shao C, Stewart V, Folkard M, Michael BD, and Prise KM (2003) Nitric oxide-mediated signaling in the bystander response of individually targeted glioma cells. *Cancer Res* **63:**8437–8442.

Shimekake Y, Nagata K, Ohta S, Kambayashi Y, Teraoka H, Kitamura K, Eto T, Kangawa K, and Matsuo H (1995) Adrenomedullin stimulates two signal transduction pathways, cAMP accumulation and Ca^{2+} mobilization, in bovine aortic endothelial cells. *J Biol Chem* **270:**4412–4417.

Shou Y, Li L, Prabhakaran K, Borowitz JL, and Isom GE (2004) Calcineurin-mediated Bad translocation regulates cyanide-induced neuronal apoptosis. *Biochem J* **379:**805–813.

Taylor GM, Meeran K, O'Shea D, Smith DM, Ghatei MA, and Bloom SR (1996) Adrenomedullin inhibits feeding in the rat by a mechanism involving calcitonin gene-related peptide receptors. *Endocrinology* **137:**3260–3264.

Taylor MM, Baker JR, and Samson WK (2005) Brain-derived adrenomedullin controls blood volume through the regulation of arginine vasopressin production and release. *Am J Physiol Regul Integr Comp Physiol* **288:**R1203–R1210.

Xia CF, Yin H, Borlongan CV, Chao J, and Chao L (2006) Postischemic infusion of adrenomedullin protects against ischemic stroke by inhibiting apoptosis and promoting angiogenesis. *Exp Neurol* **197:**521–530.

Xu Y and Krukoff TL (2004a) Adrenomedullin in the rostral ventrolateral medulla increases arterial pressure and heart rate: roles of glutamate and nitric oxide. *Am J Physiol Regul Integr Comp Physiol* **287:**R729–R734.

Xu Y and Krukoff TL (2004b) Decrease in arterial pressure induced by adrenomedullin in the hypothalamic paraventricular nucleus is mediated by nitric oxide and GABA. *Regul Pept* **119:**21–30.

Xu Y and Krukoff TL (2005) Adrenomedullin stimulates nitric oxide release from SK-N-SH human neuroblastoma cells by modulating intracellular calcium mobilization. *Endocrinology* **146:**2295–2305.

Xu Y and Krukoff TL (2006) Adrenomedullin in the rostral ventrolateral medulla inhibits baroreflex control of heart rate: a role for protein kinase A. *Br J Pharmacol* **148:**70–77.

Address correspondence to: Dr. Teresa L. Krukoff, Department of Cell Biology, Center for Neuroscience, Faculty of Medicine and Dentistry, University of Alberta, Edmonton, AB, Canada T6G 2H7. E-mail: teresa.krukoff@ualberta.ca